Cloud–Edge–End CF–MMIMO for UAV Swarms: Integrated Sensing and Robust Interference Detection in Perception Networks

Jian Sun, Dongxuan He, *Member, IEEE*, Huazhou Hou, *Member, IEEE*, Pengguang Du, *Graduate Student Member, IEEE*, Chao Fang, *Graduate Student Member, IEEE*, Changwei Zhang, *Member, IEEE*, Wei Xu, *Fellow, IEEE*, Dongming Wang, *Member, IEEE*, and Yongming Huang, *Fellow, IEEE*

***Abstract*—With the rapid advancement of sixth-generation (6G) communications, uncrewed aerial vehicle (UAV) swarms have emerged as a key application scenario. However, their high mobility and complex electromagnetic environment pose significant communication challenges, such as frequent handovers and severe co-channel interference. Although conventional cell-free massive MIMO (CF-mMIMO) systems offer ubiquitous coverage, their high backhaul overhead and complex baseband processing limit practical deployment. To address these challenges, this paper proposes a novel cloud-edge-end architecture-based CF-mMIMO communication system to support robust communication in UAV swarm perception networks. Our designed scalable architecture leverages distributed edge units (EDUs) and user-centric distributed units (UCDUs) for collaborative processing, enabling distributed localized processing and user-centric coordination, thus supporting infinite collaboration expansion. Furthermore, we develop a hybrid signal detection scheme that combines EDU-level local minimum mean squared error estimation (MMSE) detection with UCDU-level global signal aggregation, achieving performance close to that of a centralized receiver while significantly reducing backhaul overhead. To address the problem of dynamic interference, we also propose a spatiotemporal-frequency forward continuous mean excision (FCME)-based interference detection framework. This framework effectively suppresses both narrowband and wideband interference by dynamically identifying interfered frequency bands and beams. Simulation results demonstrate that the proposed method outperforms conventional approaches in terms of signal combining and interference suppression, providing a reliable communication link for UAV swarm communications.**

***Index Terms*—UAV swarms, cloud-edge-end architecture, CF-mMIMO, interference detection, hybrid signal detection.**

I. Introduction

With the rapid evolution of sixth-generation (6G) wireless communication technologies, the demand for ultra-reliable, low-latency, and highly scalable communication systems has surged, driving the emergence of uncrewed aerial vehicle (UAV) swarms as a pivotal application scenario [1], [2], [3], [4]. UAV swarms, consisting of multiple coordinated UAVs, have demonstrated immense potential in diverse fields such as disaster rescue, environmental monitoring, military reconnaissance, and smart city management [5]. In disaster rescue operations, for instance, UAV swarms can quickly establish temporary communication networks in areas where terrestrial infrastructure is damaged, enabling real-time data transmission between rescue teams and command centers [6]. In environmental monitoring, they can cover large-scale regions to collect atmospheric, hydrological, and ecological data with high spatial and temporal resolution [7]. However, the unique characteristics of UAV swarms, including high mobility, dynamic topology changes, and complex electromagnetic environments, pose significant challenges to traditional communication systems [8]. Recent years have witnessed growing research momentum in UAV cloud–edge–end integrated cell-free massive MIMO (CF-mMIMO) systems, with focuses on architecture integration, resource optimization, and intelligent enhancement. Architecturally, the fusion of satellite-terrestrial networks with UAV-enabled CF-mMIMO has become a pivotal direction to break coverage limitations. Specifically, [9] proposed an integrated satellite-terrestrial UAV CF-mMIMO framework where UAVs act as mobile access points (APs) extending satellite coverage, and developed a successive convex approximation algorithm to maximize downlink energy efficiency (EE) under power constraints, achieving significant spectral efficiency gains with finely tuned UAV power allocation. Additionally, the integration of sensing and communication (ISAC) with UAV CF-mMIMO has attracted attention, where [10] developed an extended Kalman filtering-based tracking scheme for UAV-ISAC

Received 29 September 2025; revised 28 October 2025; accepted 20 November 2025. Date of publication 25 November 2025; date of current version 24 December 2025. This work was supported in part by the National Science Foundation of China under Grant 62571112 and in part by the Major Science and Technology Project of Jiangsu Province under Grant BG2024002. Recommended for acceptance by Dr. Weijie Yuan. *(Corresponding authors: Wei Xu; Changwei Zhang.)*

Jian Sun, Wei Xu, Dongming Wang, and Yongming Huang are with National Mobile Communications Research Laboratory, Southeast University, Nanjing 210096, China, and also with Pervasive Communication Center, Purple Mountain Laboratories, Nanjing 211111, China (e-mail: jiansun@seu.edu.cn; wxu@seu.edu.cn; wangdm@seu.edu.cn; Huangym@seu.edu.cn).

Dongxuan He is with the School of Information and Electronics, Beijing Institute of Technology, Beijing 100811, China (e-mail: dongxuanhe@bit.edu.cn).

Huazhou Hou and Changwei Zhang are with Pervasive Communication Center, Purple Mountain Laboratories, Nanjing 211111, China (e-mail: houhuazhou@pmlabs.com.cn; changwei.z@outlook.com).

Pengguang Du and Chao Fang are with the School of Information Science and Engineering, Southeast University, Nanjing 210096, China (e-mail: pgdu@seu.edu.cn; fangchao@seu.edu.cn).

Digital Object Identifier 10.1109/TNSE.2025.3637039

systems, optimizing trajectories to minimize position-velocity estimation errors, laying the groundwork for robust perception-communication co-design in cloud–edge–end networks. Traditional cellular networks, which are designed primarily for ground user equipment (UE) with relatively low mobility, face inherent limitations when supporting UAV swarms. One of the key issues is frequent handovers at cell edges. As UAVs move rapidly across different cell boundaries, the frequent handover process leads to increased latency and packet loss, severely degrading communication reliability [11]. For example, in a high-density UAV swarm scenario where dozens of UAVs are moving at speeds of up to 50 m/s, the handover rate can increase by more than 300% compared to ground UEs, resulting in a 20%–30% reduction in communication throughput [12]. Another critical challenge is severe co-channel interference. Due to the three-dimensional (3D) flight trajectory of UAVs, signals from different UAVs and base stations (BSs) are prone to overlapping in the same frequency band, leading to significant interference that further deteriorates communication quality [13], [14]. Additionally, in high-density UAV swarm scenarios, the number of UAVs can reach hundreds or even thousands, exceeding the capacity of traditional cellular networks and resulting in insufficient coverage and resource allocation conflicts.

To address these challenges, cell-free massive multiple-input multiple-output (CF-mMIMO) has emerged as a promising technology. CF-mMIMO systems consist of a large number of distributed remote radio units (RRUs) that cooperate to serve users, eliminating the concept of traditional cells [15], [16]. This distributed architecture offers several advantages. First, it provides ubiquitous coverage, as UAVs can be served by multiple RRUs simultaneously, reducing the impact of coverage holes and cell-edge effects. Second, through distributed coherent transmission and reception, CF-mMIMO can effectively mitigate inter-user interference. Theoretically, as the number of RRUs approaches infinity, inter-user interference can be completely eliminated, ensuring high communication reliability [17]. Third, CF-mMIMO systems exhibit high scalability, as additional RRUs can be easily deployed to accommodate the increasing number of UAVs in swarms [18], [19], [20]. These advantages make CF-mMIMO a potential candidate for supporting UAV swarm communications.

However, conventional CF-mMIMO implementations still suffer from several critical drawbacks that hinder their practical application in UAV swarm scenarios. One major issue is excessive fronthaul overhead. In traditional CF-mMIMO systems, all RRUs need to transmit raw or partially processed data to a centralized baseband unit (BBU) for joint signal processing. This results in a massive amount of data transmission over the fronthaul network, which not only increases the cost of network deployment but also introduces significant latency [21], [22], [23]. For example, in a CF-mMIMO system with 100 RRUs each equipped with 16 antennas, the fronthaul data rate can exceed 100 Gbps, which is difficult to support with existing fronthaul technologies [24]. Another challenge is the high complexity of distributed baseband processing. Coordinating the signal processing operations of a large number of RRUs requires sophisticated algorithms and high computational resources, making it difficult to achieve real-time processing, especially in dynamic UAV swarm scenarios [25]. Additionally, conventional CF-mMIMO systems have limited scalability in practical deployments. As the number of UAVs and RRUs increases, the computational and communication burdens on the centralized BBU grow exponentially, leading to performance degradation [26], [27].

The integration of cloud-edge-end architectures into CF-mMIMO systems provides a promising solution to address these limitations [28], [29]. Cloud-edge-end architectures decompose the traditional centralized processing into three layers: the cloud layer, the edge layer, and the end layer. The cloud layer, with its powerful computing and storage capabilities, is responsible for global resource scheduling, large-scale data processing, and algorithm training [30], [31]. The edge layer, deployed closer to the end users, performs localized data processing, real-time signal detection, and resource allocation, reducing the amount of data transmitted to the cloud and minimizing latency [32], [33]. The end layer consists of the UAVs themselves, which are equipped with lightweight communication and computing modules to collect and transmit local data [34]. By integrating this architecture into CF-mMIMO systems, we can achieve a balance between distributed efficiency and centralized coordination. Specifically, EDUs can handle localized tasks such as channel estimation and beamforming, reducing fronthaul traffic, while UCDUs can perform global signal aggregation and resource scheduling, ensuring system-wide optimality [35]. This hybrid framework not only enhances the scalability of CF-mMIMO systems but also enables seamless integration of multi-band technologies, laying the foundation for full-spectrum access in 6G networks [36], [37]. The edge distributed unit (EDU) adopts a distributed deployment architecture and directly performs localized baseband processing (such as minimum mean square error (MMSE) detection) on signals within its coverage area. This avoids the long path loss and latency caused by transmitting signals to remote central nodes, thus reducing the time consumption in the signal reception and processing phases. The centralized unit-distributed unit (UCDU) aggregates the streamlined signals preprocessed by the EDU instead of raw data. This reduces the volume of data transmitted from the edge to the center and lowers transmission latency. Meanwhile, the UCDU is only responsible for global collaborative optimization, which eliminates the computational bottleneck arising from the centralized processing of all data in a centralized architecture.

Interference management remains a critical bottleneck in UAV swarm communication. The high mobility of UAVs leads to dynamic changes in the wireless channel, resulting in time-varying interference patterns [38], [39], [40]. Additionally, the complex electromagnetic environment in which UAV swarms operate, including intentional jamming, unintentional interference from other wireless systems, and multipath fading, further exacerbates the interference problem [41], [42]. Existing anti-jamming techniques, such as frequency hopping and power control, have limitations in adapting to sudden and dynamic interference. Frequency hopping, for example, requires pre-negotiated frequency hopping patterns and may not be effective against wideband interference [43], [44]. Power control can reduce interference to some extent but may lead to a decrease in communication range and throughput [45]. Therefore, there is an urgent need for a more effective interference detection and

TABLE I
SUMMARY OF RELATED WORKS ON CLOUD-EDGE-END ARCHITECTURES IN WIRELESS COMMUNICATIONS

Ref.	Arch. Layer Focus	Key Contribution	Application Scenario	Optimization Target
[66]	Cloud	Cloud-based technique development framework for 5G RAN, shows cloud can improve adaptability and system performance over conventional RAN	5G/Next-gen RAN design	Adaptability, system performance
[68]	Edge	Edge-assisted implementation of D*-Lite for UAV swarms, offloads incremental re-routing to nearby edges	UAV swarms (real-time path planning)	Replanning latency, inter-UAV signaling
[69]	Edge	Edge resource allocation for UAV-swarm communications to minimize task processing latency	UAV swarms (edge MEC)	Processing latency
[70]	Edge	Edge-computing-enabled cell-free massive MIMO systems (edge side handles parts of CF-mMIMO processing)	CF-mMIMO	Latency, distributed processing efficiency
[71]	Cloud + Edge	Cloud–edge collaborative framework with dynamic task offloading (cloud for global scheduling/training, edge for localized real-time processing)	Wireless communication/cognitive services	Resource utilization, task-offloading efficiency, latency
[72]	Cloud + Edge	Cloud–edge collaboration for energy-efficient power control in heterogeneous networks	Heterogeneous networks	Energy efficiency, power control
This Work	Cloud + Edge + End	Cloud–edge–end CF-mMIMO with distributed-localized processing at EDUs, user-centric coordination at UCDUs, and end devices integrated, hybrid detection/aggregation	UAV swarms (perception networks)	Scalability, fronthaul overhead, interference detection

mitigation scheme that can adapt to the dynamic characteristics of UAV swarm communications.

The frequency-time-space joint interference detection method based on forward consecutive mean excision (FCME) has recently gained attention as a potential solution for dynamic interference management [46], [47]. FCME is a non-parametric spectrum detection algorithm that can dynamically identify interfered frequency bands by iteratively updating the detection threshold. By extending FCME to the time and space domains, we can construct a spatiotemporal-frequency interference detection framework that not only detects interfered frequency bands but also locates the direction of interference sources [48], [49]. Combined with angle estimation correction using sum-difference amplitude comparison, this framework can significantly improve the accuracy of interference localization, ensuring robust communication links for UAVs [50].

Against this backdrop, this paper proposes a cloud-edge-end-based CF-mMIMO communication system for UAV swarms, with the following key contributions:

- A scalable CF-mMIMO architecture is designed, leveraging EDUs and UCDUs to realize distributed-localized processing and user-centric coordination, respectively. This architecture enables infinite expansion of cooperative scales, making it suitable for large-scale UAV swarm scenarios. By decoupling the baseband processing into EDUs and UCDUs, we reduce the fronthaul overhead and computational complexity while maintaining system performance.
- A hybrid signal detection scheme is developed, combining EDU-level local MMSE detection with UCDU-level global signal aggregation. This scheme achieves near-centralized performance with significantly reduced fronthaul overhead. The local MMSE detection at the EDU level ensures real-time processing, while the global signal aggregation at the UCDU level optimizes the overall system performance.
- An FCME-based interference detection framework is proposed, integrating dynamic frequency/beam selection and angle estimation correction. This framework can effectively mitigate both narrowband and wideband interference in UAV swarm scenarios. By dynamically identifying interfered frequency bands and beams and correcting angle estimates, we improve the accuracy of interference localization and suppression, ensuring reliable communication for UAV swarms.

The remainder of this paper is organized as follows: Section II presents the related work, reviewing existing research on CF-mMIMO systems, cloud-edge-end architectures, and interference management for UAV swarms. Section III details the system architecture and signal processing models of the proposed cloud-edge-end-based CF-mMIMO system. Section IV describes the interference detection and mitigation strategies, including the FCME-based interference detection framework and angle estimation correction method. Section V provides simulation results and performance analysis to evaluate the effectiveness of the proposed system. Finally, Section VI concludes the paper and discusses future research directions.

II. RELATED WORK

A. CF-MMIMO Systems for UAV Communications

CF-mMIMO has been extensively studied in recent years for its potential to address the limitations of traditional cellular

networks in supporting UAV communications. Early research on CF-mMIMO focused on the theoretical analysis of system performance, including spectral efficiency, energy efficiency, and interference suppression [51], [52]. Ngo derived the spectral efficiency of CF-mMIMO systems in single-cell and multi-cell scenarios, showing that CF-mMIMO can achieve significantly higher spectral efficiency than traditional cellular networks. Larsson et al. [51] analyzed the energy efficiency of CF-mMIMO systems, demonstrating that the distributed architecture of CF-mMIMO can reduce the energy consumption of BSs by leveraging the diversity gain from multiple RRUs.

With the increasing interest in UAV communications, researchers have begun to explore the application of CF-mMIMO in UAV scenarios. Zeng et al. [53] studied the coverage performance of CF-mMIMO for UAVs, showing that CF-mMIMO can provide better coverage for UAVs than traditional cellular networks due to its distributed RRUs. [54] proposed a CF-mMIMO-based communication system for UAV swarms, where multiple RRUs cooperate to serve UAVs, reducing the impact of high mobility and interference. They developed a channel estimation algorithm based on pilot reuse to improve the accuracy of channel state information (CSI) acquisition, which is crucial for coherent signal processing in CF-mMIMO systems.

However, existing CF-mMIMO systems for UAV communications still face several challenges. One of the main issues is the high fronthaul overhead. In [53] and [54], the authors assumed that all RRUs transmit raw data to a centralized BBU, which results in a large amount of fronthaul traffic. To address this problem, some researchers have proposed fronthaul compression techniques. Kim et al. [55] proposed a compressive sensing-based fronthaul compression scheme for CF-mMIMO systems, reducing the fronthaul data rate by compressing the CSI and received signals. Wang et al. [56] developed a distributed compression algorithm that enables RRUs to compress the received signals locally before transmitting them to the BBU, further reducing the fronthaul overhead.

Another challenge is the dynamic topology of UAV swarms. As UAVs move, the association between UAVs and RRUs changes dynamically, requiring efficient resource allocation and handover mechanisms. Guo et al. [57] proposed a dynamic RRU association algorithm for CF-mMIMO-based UAV communication systems, where UAVs are associated with RRUs based on their location and channel quality. The algorithm adaptively adjusts the RRU association to minimize interference and maximize system throughput. Zaher et al. [58] developed a handover management scheme for CF-mMIMO systems, which reduces handover latency by pre-establishing communication links with neighboring RRUs.

B. Cloud-Edge-End Architectures in Wireless Communications

Cloud-edge-end architectures have emerged as a promising paradigm for wireless communications, enabling the integration of cloud computing, edge computing, and end-device computing to meet the diverse requirements of different applications [59], [60], [61]. In cloud computing, the cloud layer provides centralized computing and storage resources, which are suitable for large-scale data processing and algorithm training [62], [63]. For example, in [62], the authors proposed a cloud-based technique development framework for 5G radio access networks, which demonstrates the potential of cloud architectures to improve system adaptability and performance compared with conventional RAN designs.

Edge computing, on the other hand, deploys computing resources closer to the end users, reducing the latency of data transmission and processing [64], [65]. Lee et al. [64] design an edge-assisted implementation of the D $*$ Lite algorithm for UAV swarms, offloading incremental path updates to nearby edge nodes to handle dynamic obstacles and link disruptions in real time. Their architecture couples on-board sensing with distributed planning at the edge, yielding lower end-to-end replanning latency and reduced inter-UAV signaling compared with purely on-board routing. Hu et al. [66] developed an edge resource allocation algorithm for UAV swarm communications, which optimizes the allocation of edge computing resources to minimize the processing latency of UAV tasks.

The integration of cloud and edge computing has also been studied to achieve a balance between centralized and distributed processing. Ding et al. [67] proposed a cloud-edge collaborative framework for wireless communication systems, where the cloud is responsible for global resource scheduling and algorithm training, and the edge performs localized data processing and real-time decision-making. They developed a task offloading algorithm that dynamically offloads tasks from end devices to the edge or cloud based on the task requirements and resource availability. Zhang et al. [68] studied the energy efficiency of cloud-edge collaborative systems, showing that by optimally offloading tasks, the energy consumption of end devices can be significantly reduced.

To facilitate a side-by-side comparison, Table II summarizes representative cloud–edge–end architectures in wireless communications.

C. Interference Management for UAV Swarm Communications

Interference management is a critical issue in UAV swarm communications, and various techniques have been proposed to mitigate interference. Frequency hopping is one of the most widely used anti-jamming techniques, where the transmitter and receiver switch between different frequency bands according to a pre-defined pattern [3], [69]. Xue et al. [70] proposed a adaptive frequency hopping scheme for UAV swarm communications, which dynamically adjusts the frequency hopping pattern based on the interference environment. The scheme uses a cognitive-based high robust algorithm to detect the interference frequency bands and avoids using them, improving the anti-jamming performance.

Power control is another effective technique for interference mitigation. By adjusting the transmit power of UAVs and BSs, the interference to other users can be reduced [71], [72]. Shen et al. [71] formulate a joint trajectory and power control problem for maximizing the aggregate sum rate of the UAV-interference channel for a given flight interval, under practical constraints

TABLE II
COMPARISON CHART OF CORE INDICATORS BETWEEN CENTRAL AND PERIPHERAL REGIONS

Airspace	Uplink Throughput	Uplink Bit Error Rate	Uplink MCS	Uplink SINR
Center	240.67	0	28	28.4
Edge	122.45	10.5	21	13.5

on the UAV flying speed, altitude, and collision avoidance. Neetu et al. [72] developed a power control scheme for CF-mMIMO-based UAV communication systems, which maximizes the signal-to-interference-plus-noise ratio (SINR) among the UEs and minimizes the power consumption by optimizing the transmit powers of UAV-APs.

Beamforming is also widely used in UAV swarm communications to focus the signal energy on the desired UAVs and reduce interference to other users [73], [74], [75]. Miao et al. [73] proposed a 3D beamforming algorithm for UAV swarm communications, which optimizes the azimuth and elevation angles of the beamforming vectors to improve the coverage and SINR of UAVs. They considered the 3D flight trajectory of UAVs and dynamically adjusted the beamforming vectors to track the UAVs. Wang et al. [75] proposed a digital beamforming method based on signal eigen-subspace to effectively suppress interference and avoid attenuation of the desired signal.

In addition to these interference mitigation techniques, researchers have also explored the use of advanced signal processing and machine learning techniques for interference detection and mitigation. FCME, as a non-parametric spectrum detection algorithm, has been used for dynamic interference detection [76], [77], [78]. Vuohtoniemi et al. [76] proposed an FCME-based interference detection scheme for power line communication systems, which can dynamically identify the occupied frequency bands by primary users. Zhang et al. [78] proposed to add a joint judgment of medium threshold and high threshold on the basis of the original low threshold to improve the detection accuracy, and reduce the computational complexity of the original scheme by adopting different strategy.

Machine learning techniques have also been applied to interference management for UAV swarm communications. Wang et al. [79] proposed a dual-input interference recognition network (DIRNet) with a few model parameters, incorporating deep features extracted based on the data-driven approach and manual features designed based on expert knowledge. Hosseini et al. [80] proposed a novel jamming detection algorithm which has a hybrid structure of simple classification and anomaly detection models, thus can classify known attacks used for training and detect unknown attacks not used for training.

D. Summary of Related Work

Although significant progress has been made in the research of CF-mMIMO systems, cloud-edge-end architectures, and interference management for UAV swarms, there are still several gaps that need to be addressed. First, existing CF-mMIMO systems for UAV communications have high fronthaul overhead and computational complexity, which limit their scalability in large-scale UAV swarm scenarios. Second, the integration of cloud-edge-end architectures into CF-mMIMO systems is still in its early stages, and there is a lack of efficient resource allocation and task offloading mechanisms that can adapt to the dynamic characteristics of UAV swarms. Third, existing interference management techniques are not fully adapted to the dynamic and complex interference environment of UAV swarms, and there is a need for more effective interference detection and mitigation schemes that can handle both narrowband and wideband interference.

To fill these gaps, this paper proposes a cloud-edge-end-based CF-mMIMO communication system for UAV swarms. The proposed system leverages the advantages of cloud-edge-end architectures to reduce fronthaul overhead and computational complexity, and develops a hybrid signal detection scheme and an FCME-based interference detection framework to improve system performance and interference suppression capabilities.

III. DESIGN OF THE PROPOSED CF-MMIMO SYSTEM

A. New Cloud-Edge-End Cell-Free Radio Access Network Architecture

Traditional cell-free MIMO systems, characterized by their distributed architecture, demonstrate significant advantages in both system performance and deployment flexibility. Firstly, coherent reception is implemented locally at each RRU, eliminating the need for inter-RRU channel information exchange. This approach substantially reduces coordination complexity, latency, and reliability risks associated with cross-RRU synchronization. Secondly, such systems exhibit theoretical superiority in interference suppression. Even with a simple channel-conjugate multiplication-based coherent reception scheme, as the number of RRUs approaches infinity, inter-UAV interference is progressively mitigated, leading to asymptotically complete interference elimination in theory. This provides robust communication quality in high-interference scenarios. Thirdly, the architecture supports strong scalability. With fronthaul network support, UAV signal combining can be performed across multiple BBUs, removing constraints on the number of RRUs and UAVs and enabling arbitrary system expansion. This allows the cell-free architecture to adapt to varying capacity requirements across diverse scenarios. Moreover, compared to centralized or partitioned architectures such as small-cell systems, traditional cell-free MIMO improves signal quality for edge users (or edge UAVs) through distributed multi-RRU coverage. This reduces performance fluctuations caused by cell-boundary effects and enhances overall system fairness and communication stability.

To further improve the performance of the cell-free MIMO system, in this paper, we propose a novel CF-RAN structure. As is illustrated in Fig. 3, the novel cloud-edge-end CF-RAN architecture comprises RRUs, EDUs, a UCDU, and a

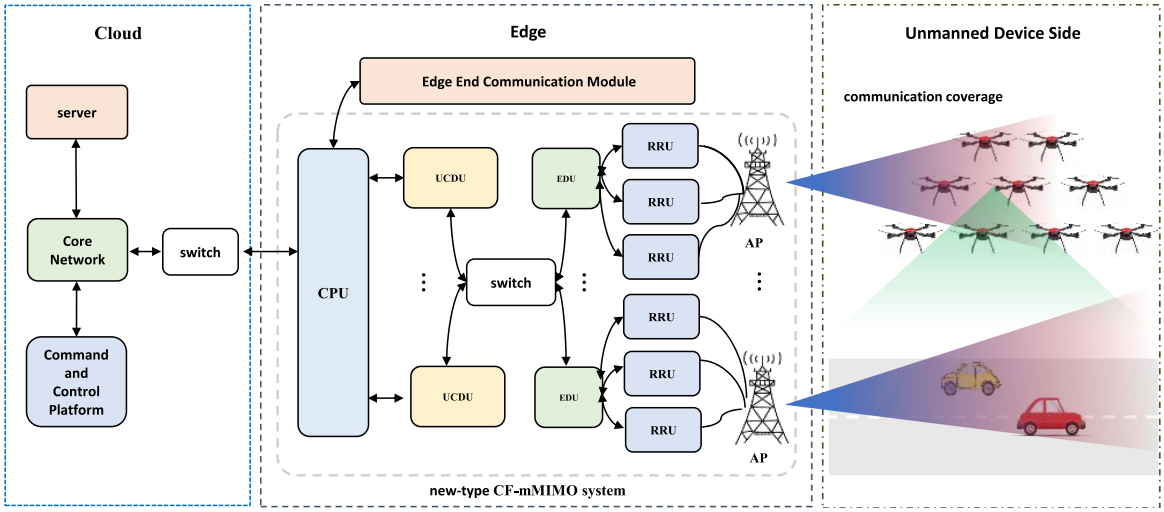

Fig. 1. The cloud-cdge-cnd cell-cree cireless access network architecture.

centralized control unit. Each multi-antenna RRU performs RF transmission/reception and digital/analog conversion. Each EDU, connected to multiple RRUs, handles baseband processing including channel estimation, multi-UAV/multi-stream detection/precoding, and calibration signal extraction. The UCDU, linked directly or via switches to multiple EDUs, performs cooperative physical-layer processing: merging uplink data streams from EDUs, distributing downlink streams, and estimating inter-RRU channels. The centralized control unit, connected to UCDUs directly or through switches, determines the data stream mapping between EDUs and UCDUs.

A key feature is the functional split between EDU and UCDU at the data stream level—spatial streams over the same time-frequency resources. The transmit split occurs after forward error correction (FEC) encoding but before precoding; the receive split follows multi-stream/multi-UAV detection but precedes FEC decoding. Under centralized control, all uplink streams of a UAV are routed from multiple EDUs to one UCDU, and downlink streams are distributed from that UCDU to EDUs, using an enhanced common public radio interface (eCPRI) for data exchange. As shown in Fig. 1.

The control unit associates UAVs with RRUs/EDUs/UCDU based on location or channel priors, adhering to the principle of one UAV per UCDU while balancing UCDU load and minimizing cross-switch access.

In this experiment, the constructed system comprises 8 RRUs (model: 4T4R, 3.5 GHz), which are connected to 4 EDUs (model: H3C 6900 servers) to support localized MMSE detection for 1–9 UAVs. Additionally, 2 UCDUs (model: H3C 4900 servers) are deployed to perform global aggregation, thus mitigating fronthaul overload. Regarding the energy consumption of the equipment, each EDU, UCDU, and RRU consumes 15 W, 35 W, and 8 W, respectively.

In summary, the innovations of this CF-RAN architecture include:

1. A scalable structure supporting 6G UAV-centric access via distributed EDU and cloud-cooperative UCDU baseband pooling, enabling unlimited cooperative scaling;
2. Functional separation: EDUs perform local processing without inter-EDU channel exchange, while UCDUs perform UE-centric data merging conducive to cloud-pooling, ensuring scalability;
3. EDU handles frequency-dependent functions (e.g., channel estimation, beamforming), while UCDU implements frequency-agnostic modulation/coding, enabling software-defined multi-band integration. Thus, it constitutes a full-spectrum cell-free RAN.

B. System Modeling

1) Cloud Communication Module: The cloud communication module comprises four key components: the core network, cloud servers, a command and control platform, and switches. The switch serves as the communication hub, facilitating internal data exchange and physical connectivity among the core network, cloud servers, and command platform, while also establishing links and forwarding data to edge nodes. The core network acts as the gateway for data entering and exiting the cloud, enabling bidirectional data flow between the edge and cloud. Cloud servers form the computational core, executing critical tasks such as algorithm training and inference. The command and control platform functions as the management center, ensuring efficient operation of server resources and tasks through real-time monitoring and dynamic scheduling. These components operate interdependently to form a highly efficient and reliable cloud computing ecosystem, providing essential support for data processing, task execution, and edge collaboration.

Within the cloud computing environment, core functionalities include algorithm model training, real-time inference, task execution, and data transmission. Algorithm training leverages high-performance computing resources to optimize model parameters through iterative processing of large-scale datasets. Real-time inference employs trained models to generate predictions rapidly upon receiving new data, requiring low latency and high throughput. Task execution incorporates

flexible scheduling mechanisms for resource management, enabling efficient parallel processing and fault tolerance. Data transmission ensures secure and format-compatible cross-system communication. Additionally, resource monitoring and scheduling tools track system usage and dynamically adjust allocations. Task monitoring modules oversee job status to ensure prompt fault handling. Data storage management involves selecting appropriate storage types and implementing backup strategies to prevent data loss. Network monitoring continuously evaluates performance to guarantee efficient and secure data transmission. These integrated functionalities collectively establish a robust and high-performance cloud computing ecosystem.

2) Edge Communication Module: The edge communication module comprises a UCDU, EDUs, RRUs, APs, and a CPU. Each unit performs distinct yet tightly coordinated functions. RRUs interact with UAV-mounted transceivers via wireless links for uplink reception and downlink transmission. The UCDU demodulates received signals from RRUs—converting modulated RF signals to baseband—and modulates outgoing baseband signals, in addition to performing channel encoding/decoding. EDUs dynamically allocate baseband processing resources based on service demands, distributing tasks across nodes for specialized operations such as channel coding or signal demodulation. RRUs also upconvert UCDU-supplied baseband signals to the target RF band via mixing; in swarm scenarios, this shifts signals to higher frequencies suitable for long-range transmission.

In the edge computing environment, this module enables centralized management of UAV swarms by collecting real-time data on status, location, and task priority. It optimizes resource allocation, monitors system metrics (e.g., resource usage, task progress, data traffic), and dynamically enhances communication efficiency between edge nodes.

In the scenario of a UAV communication system, it is assumed that there is no communication interaction between the UAV in the system, so the tasks of each UAV are independent. In addition, each UAV is provided with communication services by N APs, and each AP is equipped with N_t antennas. The specific implementation details of uplink and downlink transmission are described as follows:

1) Uplink Phase: In the uplink phase, the signal received by the n-th AP can be expressed as:

$$y_n = \sum_{k=1}^{K} h_{k,n} x_k + z_n, \tag{1}$$

where $h_{k,n} \in \mathbb{C}^{N_1 \times 1}$ represents the channel coefficient between the k-th UAV and the n-th AP, x_k represents the transmit signal of the k-th UAV, and z_n represents the additive white Gaussian noise (AWGN) with power σ^2 at the n-th AP.

By using the detector $v_{k,n}$ at the n-th AP, the transmit signal of the k-th drone can be obtained through collaborative detection:

$$\hat{x}_k = \sum_{n=1}^{N} I_{k,n} v_{k,n}^H y_n, \tag{2}$$

where $I_{k,n} \in \{0, 1\}$ is an indicator function, which is 1 if and only if the k-th UAV is served by the n-th AP.

In a fully distributed architecture, each AP is limited to acquiring local CSI, i.e., $h_{k,n}$, thus performing non-cooperative signal detection (e.g., conventional maximum ratio combining (MRC)). This decentralized strategy inevitably leads to significant performance degradation, while full cooperation results in excessive fronthaul overhead.

To address this challenge, following the CF-mMIMO architecture, multiple APs are interconnected with dedicated EDUs for signal detection. This configuration improves cooperative processing performance by integrating additional cooperative APs while maintaining system scalability. Specifically, each drone can be associated with multiple EDUs but only with one UCDU. After demultiplexing the multi-drone data streams, the EDUs forward them to the associated UCDU, and the UCDU performs signal aggregation from distributed EDUs. The composite partial minimum mean square error (P-MMSE) detector at the m-th EDU is formulated as:

$$v_{m,k} = p_k \left[\sum_{i \in \mathcal{A}_m} p_i \bar{h}_{i,m} \bar{h}_{i,m}^H + \sigma^2 I \right]^{-1} \bar{h}_{k,m}, \tag{3}$$

where P_k represents the transmit power of the k-th UAV, $\mathcal{A}_m$ denotes the set of UAVs associated with the m-th EDU, and $\bar{h}_{i,m}$ represents the equivalent channel between the i-th UAV and the m-th EDU.

2) Downlink Phase: In the downlink phase, the received signal at the k-th UAV is expressed as:

$$y_k = \sum_{m=1}^{M} \bar{h}_{k,m}^H \left(\sum_{i \in \mathcal{A}_m} w_{i,m} x_i \right) + z_k \tag{4}$$

where y_k represents the signal received by the k-th drone, corresponding to the signal acquisition process of terminal-layer devices in the CF-mMIMO architecture. $\sum_{m=1}^{M} \bar{h}_{k,m}^H$ represents the conjugate transpose of the equivalent channel coefficients between the k-th drone and the m-th EDU. In CF-mMIMO, distributed EDUs cooperate with the CPU through optical fiber links to achieve coherent joint transmission (CJT) of multi-drone signals. $\bar{h}_{k,m}$ reflects the time-varying characteristics and spatial fading features of the channel. $\sum_{i \in \mathcal{A}_m} w_{i,m} x_i$ indicates that the m-th EDU performs precoding processing on the signals of the associated drones (set $\mathcal{A}_m$). Here, x_i is the transmit signal of the i-th UAV. $w_{i,m}$ represents the precoding vector at the m-th EDU for the k-th UAV. Similarly, the downlink data stream of the same drone is specifically transmitted from the UCDU to multiple EDUs, achieving downlink CJT through coordinated beamforming among distributed EDUs; $\mathcal{A}_m$ is the set of drones associated with the m-th AP, z_k is the additive noise at the k-th UAV, M is the number of APs or cooperative nodes, and ^{H} denotes the conjugate transpose operation. In signal processing, the conjugate transpose of the channel matrix is often used to adapt to algorithm requirements, facilitating coherent combining of signals and interference suppression.

3) UAV Swarm Terminal Module: The UAV swarm terminal module comprises multiple UAVs, each equipped with a flight control unit (FCU), terminal processor, and communication

unit. The FCU acquires real-time state data including position, velocity, and attitude. The terminal processor handles mission-specific data processing, such as preliminary analysis of camera-captured video streams. Processed results and real-time state data are transmitted via the communication module to edge and cloud servers for subsequent management, analytical operations, and decision optimization. In this implementation, the proposed cloud-edge-end architecture offloads computational tasks from UAVs to ground servers, significantly reducing computational energy consumption and enhancing operational endurance.

The UAV swarm operates without direct inter-UAV communication, with all communications routed through base stations. Data exchange between UAVs employs the user datagram protocol (UDP), where each UAV uploads its state information to cloud servers, which aggregate and redistribute the data via UDP broadcasts.

4) Signal Reception Design for Communication Architecture: In traditional architectures, each base station employs an independent receiver, with UAV communicating solely with the nearest base station. This approach frequently results in issues such as frequent handovers, signal interference, and rate degradation when UEs are located at cell edges, indoor obstructed areas, or high-density scenarios.

The edge communication module addresses these limitations by deploying numerous APs distributed over a wide area. This strategy significantly mitigates the impact of large-scale fading on communication performance and increases the degrees of freedom in wireless channels.

Leveraging the scalable nature of distributed signal processing while balancing system performance and implementation complexity, the edge communication module achieves performance comparable to centralized receivers. Notably, only statistical channel information needs to be transmitted between EDUs and the CPU via fronthaul links.

During the communication process of unmanned systems, signal acquisition is first jointly completed by the RRU and AP. Specifically, the RRU is responsible for receiving signals transmitted back by remote unmanned systems, while the AP supplements this by receiving cellular signals. Serving as signal "entrances", the two devices transmit the original signals to the EDU.

Then, the edge preprocessing phase begins, the EDU performs simple processing on the received original signals, eliminating minor interference and organizing signal formats. After completion, it transmits the processed signals to the UCDU. Next, the UCDU undertakes the centralized processing task. It collects the preprocessed signals from multiple EDUs, conducts centralized integration—including combining multi-path signals and reducing interference—and simultaneously generates a downlink signal strategy for the UAVs. Subsequently, it synchronizes the processing results and UAV status to the CPU.

Based on this information, the CPU carries out global scheduling work: It allocates global resources according to the data received from the UCDU and feeds back the generated scheduling instructions to the UCDU. Finally, the signal return phase commences: In accordance with the CPU's instructions, the UCDU transmits the final downlink signal strategy to the EDU, which then forwards the signal to the RRU and AP. Ultimately, the RRU or AP sends the signal to the unmanned system, thereby completing a full communication cycle.

The UCDU can receive identical uplink data from multiple EDUs for a single drone. Maximum ratio combining or MMSE algorithms enhance signal-to-noise ratio. The MMSE detection vector v_k^{MMSE}, computed at the CPU, is partitioned into segments distributed to subordinate EDUs. These segments correspond to the number and indices of APs managed by each EDU. Thus, EDUs utilize v_k^{MMSE} segments for local signal detection, while the CPU combines detected signals from all EDUs. This approach achieves equivalent performance to direct CPU-based detection using v_k^{MMSE} across all EDU received signals [81], [82]. As shown in Table I.

5) System Flight Data: During the system flight test process, we used the AIRtracer software to conduct real-time monitoring of communication data, including important metrics such as uplink throughput rate, uplink bit error rate, uplink modulation and coding scheme(MCS), and signal-to-interference-plus-noise ratio(uplink SINR),As shown in Figs. 2 and 3. Among the test scenarios, the information from the central area and edge area of the flight formation composed of 9 aircraft was also recorded for comparison,As shown in Table II.

IV. Interference Detection Method Based on Spatiotemporal-Frequency FCME

A novel CF-RAN has been designed and modeled in the previous sections, establishing a hierarchical collaborative architecture of "RRU-EDU-UCDU-centralized control unit". This architecture clearly defines the functional division of each unit, including RF transceiver, localized baseband processing, and global scheduling. However, this architecture still faces bottlenecks in practical scenarios: high UAV mobility causes dynamic interference, narrowband/wideband interference randomly occurs in complex electromagnetic environments, traditional anti-interference techniques (frequency hopping, power control) are difficult to adapt, and although the architecture has theoretical potential for interference suppression, it lacks precise interference sensing and localization mechanisms.

Towards this end, this section proposes an interference sensing and detection method based on spatio-temporal-frequency FCME. Specifically, this method utilizes the multi-AP spatio-temporal-frequency signal acquisition capability and EDU's localized preprocessing function, adopting frequency-domain FCME to identify interfered frequency bands and beam-domain FCME to locate interference directions. Finally, a three-dimensional spatio-temporal-frequency interference sensing system is constructed. This approach compensates for the shortcomings of interference management in novel cell-free systems and achieves collaborative optimization of architectural performance and anti-interference capability.

For the receiver, the received time-domain signal is a matrix of size $N_b \times L$, where L represents the time series length and N_b represents the number of beam training pairs between the

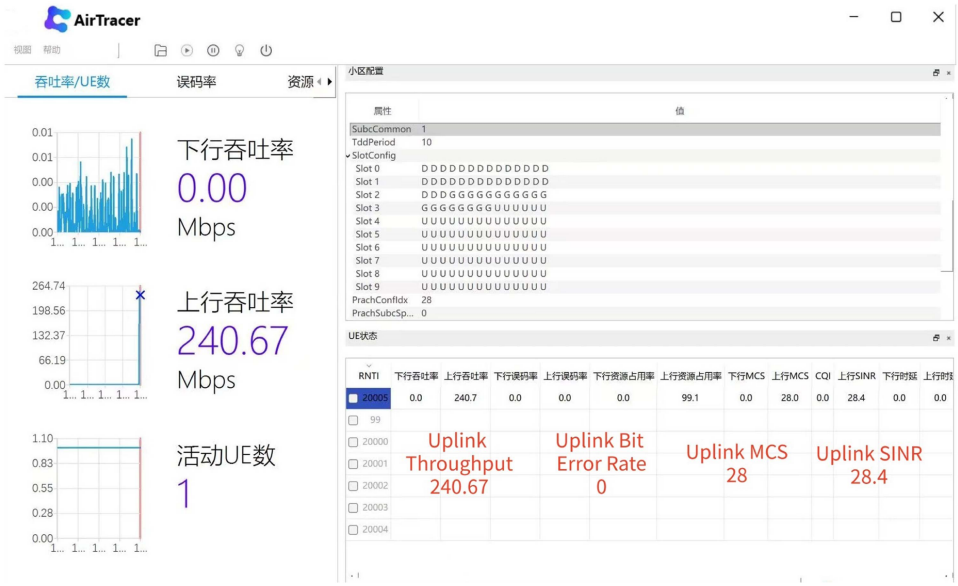

Fig. 2. Uplink core data in the central area.

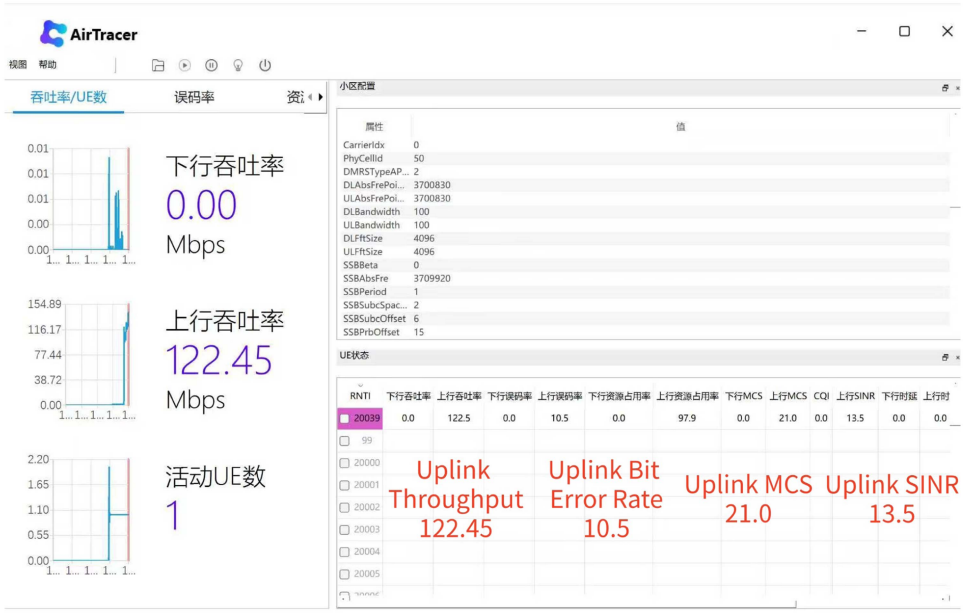

Fig. 3. Uplink core data in the edge area.

receiver and users. For interference detection, we project the received signal onto unused pilots in the system, where the received signal contains only interference and simple noise. The time-domain signal is first transformed into the frequency-domain signal through a K-point fast fourier transform (FFT). At this point, spectrum detection can be simply regarded as a binary hypothesis problem. First, for the k-th frequency point, the hypothesis test is defined as:

$$\mathcal{H}_0 : y_{n,k} = n_{n,k}, \quad n = 1, \ldots, N_b, \tag{5}$$

$$\mathcal{H}_1 : y_{n,k} = s_{n,k} + n_{n,k}, \quad n = 1, \ldots, N_b, \tag{6}$$

where $y_{n,k}$ represents the observation at the k-th frequency point of the n-th beam pair, $n_{n,k}$ is additive white Gaussian noise following $\mathcal{CN}(0, \sigma^2)$, $s_{n,k}$ represents the independent interference signal, and $\mathcal{H}_0$ and $\mathcal{H}_1$ represent the absence and presence of interference, respectively.

Let the detection statistic at the k-th frequency point be expressed as:

$$Q_k = \frac{1}{N_b} \sum_{n=1}^{N_b} |y_{n,k}|. \tag{7}$$

Under the $\mathcal{H}_0$ hypothesis, $|y_{n,k}|$ follows a Rayleigh distribution with probability density function:

$$f_{|y_{n,k}|}(y) = \frac{2y}{\sigma^2} e^{-\frac{y^2}{\sigma^2}}, \quad y > 0, \tag{8}$$

with mean and variance given by $\mathbb{E}(|y_{n,k}|) = \sigma\frac{\sqrt{\pi}}{2}$ and $\mathrm{Var}(|y_{n,k}|) = \sigma^2\frac{4-\pi}{4}$, respectively.

When the sample size N_b is large, by the central limit theorem, the statistic Q_k approximately follows a normal distribution:

$$Q_k \sim \mathcal{N}\left(\sigma\frac{\sqrt{\pi}}{2}, \sigma^2\frac{4-\pi}{4N_b}\right). \tag{9}$$

The relationship between the false alarm rate P_f and the threshold η is given by $P_f = Q(\frac{\eta-\sigma\frac{\sqrt{\pi}}{2}}{\sigma\sqrt{\frac{4-\pi}{4N_b}}})$, therefore

$$\eta = \sigma\sqrt{\frac{4-\pi}{4N_b}}Q^{-1}(P_f) + \sigma\frac{\sqrt{\pi}}{2}. \tag{10}$$

According to the constant false alarm rate threshold design formula, $\eta = \gamma\mathbb{E}(Q_k)$, where $\mathbb{E}(Q_k)$ represents the expected value of the detection statistic and γ is the threshold factor, we obtain:

$$\gamma = \frac{\eta}{\mathbb{E}(Q_k)} = \sqrt{\frac{4-\pi}{N_b\pi}}Q^{-1}(P_f) + 1. \tag{11}$$

In the following, we perform frequency point detection based on FCME, which is a spectrum detection algorithm that iteratively updates the threshold and cyclically classifies frequency points until stability is achieved. Initially, the algorithm sets two sets: interfered and non-interfered, placing the smallest portion of the sorted statistics into the non-interfered set. Then, through iterative operations, it continuously verifies the threshold, removes low-amplitude samples from the interfered set, and adds them to the non-interfered set, and updates the threshold until the classification of frequency points stabilizes. The FCME-based frequency point detection algorithm is as follows:

Step 1: First, sort the detection statistics at K frequency points in ascending order: $Q_{k_1} < Q_{k_2} < \ldots < Q_{k_K}$. Select T frequency points with the smallest statistics from the sorted list, place these frequency points corresponding to this portion of statistics into the initial non-interfered set $F = \{k_1, k_2, \ldots, k_T\}$, and place the remaining frequency indices into set $\bar{F} = \{k_{T+1}, \ldots, k_K\}$. Calculate the mean of the detection statistics corresponding to the frequency points in set F, i.e., $E_F = \frac{1}{|F|}\sum_{k\in F} Q_k$, where $|F|$ is the cardinality of set F. Initially, $|F| = T$ indicates that the selected T frequency points are not interfered.

Step 2: Update the threshold according to the formula $\eta = \gamma E_F$. Due to the instability of noise power, false alarms are likely to occur, so an auxiliary variable offset is added to control the threshold, i.e., set $\eta = \gamma E_F +$ offset. Then compare it with the detection values at all frequency points. If $Q_k < \eta$, decide that the frequency point is not interfered, remove k from $\bar{F}$, and add k to set F.

Step 3: Update the mean of set F: $E_F = \frac{1}{|F|}\sum_{k\in F} Q_k$, and jump to Step 2.

Step 4: Iterate Steps 2 and 3 until set F stabilizes, or the maximum number of iterations is reached, then end the iteration.

Step 5: Provide the threshold value for the decision of frequency point detection, and based on the final threshold, decide the interference situation, outputting the set of interfered frequency points $\bar{F}$.

After implementing FCME-based frequency point detection, the detection problem for the n-th beam can be constructed as:

$$\mathcal{H}_0 : y_{n,k} = n_{n,k}, \quad k \in F, \tag{12}$$

$$\mathcal{H}_1 : y_{n,k} = s_{n,k} + n_{n,k}, \quad k \in F. \tag{13}$$

At this point, the detection statistic for the n-th beam can be constructed based on the frequency-domain detection results as:

$$P_n = \frac{1}{|F|}\sum_{k\in F}|y_{n,k}|. \tag{14}$$

Similarly, when the sample size $|F|$ is large, according to the central limit theorem, the statistic P_n approximately follows a normal distribution, so the threshold factor can be obtained as:

$$\gamma' = \sqrt{\frac{4-\pi}{|F|\pi}}Q^{-1}(P_f) + 1. \tag{15}$$

The algorithm flow for FCME-based beam detection is as follows:

Step 1: Sort the detection statistics at N_b beams in ascending order: $P_{n_1} < P_{n_2} < \ldots < P_{n_{N_b}}$. From the sorted beams, select L items with the smallest statistics, place the beam indices corresponding to this portion of statistics into the initial non-interfered beam set $B = \{n_1, n_2, \ldots, n_L\}$, and place the remaining beam indices into set $\bar{B} = \{n_{L+1}, \ldots, n_{N_b}\}$. Calculate the mean of the detection statistics corresponding to the beams in set B, i.e., $E_B = \frac{1}{|B|}\sum_{n\in B} P_n$, where $|B|$ is the cardinality of set B.

Step 2: Update the threshold according to the formula $\eta' = \gamma' E_B +$ offset. Then compare it with the detection values at all beams. If $P_n < \eta'$, decide that the beam is not interfered, remove n from $\bar{B}$, and add n to set B.

Step 3: Update the mean of set B: $E_B = \frac{1}{|B|}\sum_{n\in B} P_n$, and jump to Step 2.

Step 4: Iterate Steps 2 and 3 until set B stabilizes, or the maximum number of iterations is reached, then end the iteration.

Step 5: Provide the final threshold value for the beam detection decision, and based on the final threshold, decide the interference situation, outputting the set of interfered beams $\bar{B}$.

Step 6: Based on the beam scanning pattern, determine the elevation and azimuth angle indices corresponding to the elements in the beam set, and feed them back to the angle estimation module.

If interference is detected based on FCME, then angle information for both interference and users needs to be estimated at the interfered frequency points and beam points. For an interfered frequency point k and beam point n, the corresponding beam scanning DFT codeword can be determined, thereby obtaining the initial angle estimate of the interferer. To further improve the accuracy of angle measurement, this scheme proposes an angle estimation algorithm based on sum-difference amplitude ratio correction. It uses the ratio information between the power peak and adjacent peak amplitudes in the beam-domain received signal to estimate the angle deviation value, and then corrects the initial angle estimate based on the deviation estimate.

The principle of estimating angle deviation using the sum-difference amplitude ratio method is shown in Fig. 4. Let the beam point where interference is detected be n_1, and the beam

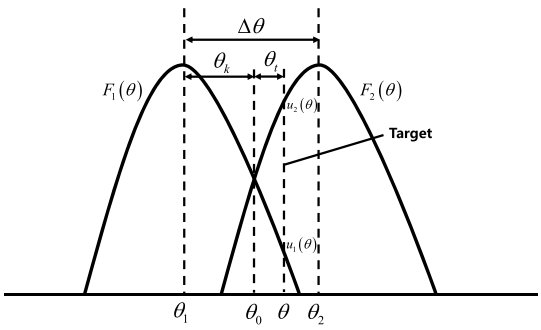

Fig. 4. Schematic diagram of angle deviation estimation using sum-difference amplitude ratio method.

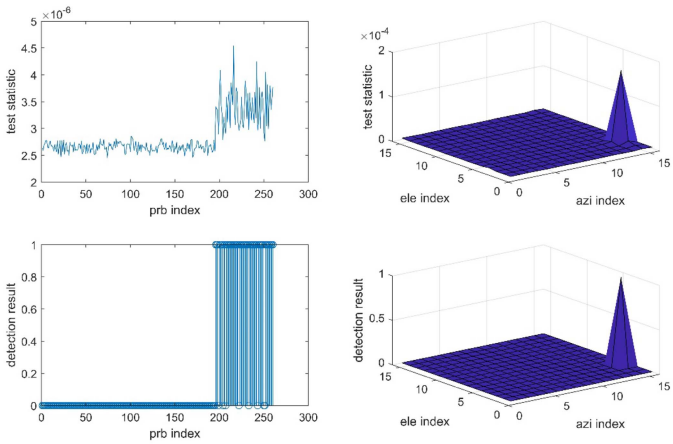

Fig. 5. Interference detection performance in anti-jamming scenario.

point corresponding to the larger beam-domain received signal adjacent to n_1 be n_2. The beam patterns corresponding to beam points n_1 and n_2 are $F_1(\theta)$ and $F_2(\theta)$, respectively. The two beam pointing directions and the equal-signal axis direction are denoted as θ_1, θ_2, and θ_0, respectively, satisfying $\theta_2 - \theta_0 = \theta_0 - \theta_1 = \theta_k = \Delta\theta/2$. Then we have:

$$F_1(\theta) = F(\theta - \theta_1) = F(\theta + \theta_k - \theta_0), \tag{16}$$

$$F_2(\theta) = F(\theta - \theta_2) = F(\theta - \theta_k - \theta_0). \tag{17}$$

Assuming the true target angle is θ, and denoting the difference between the true angle and the equal-signal axis angle as $\theta_t = |\theta - \theta_0|$, then the beam-domain received signals at the two beam points are:

$$u_1(\theta_t) = WF(\theta_t + \theta_k), \tag{18}$$

$$u_2(\theta_t) = WF(\theta_t - \theta_k). \tag{19}$$

where W is the amplitude coefficient, related to transceiver antenna parameters, target distance, and other factors. Thus, the sum beam received signal $u_\Sigma(\theta_t)$ and difference beam received signal $u_\Delta(\theta_t)$ can be obtained as:

$$u_\Sigma(\theta_t) = u_1(\theta_t) + u_2(\theta_t) = W[F(\theta_t + \theta_k) + F(\theta_t - \theta_k)], \tag{20}$$

$$u_\Delta(\theta_t) = u_1(\theta_t) - u_2(\theta_t) = W[F(\theta_t + \theta_k) - F(\theta_t - \theta_k)]. \tag{21}$$

where $F_\Sigma(\theta_t) = F(\theta_t + \theta_k) + F(\theta_t - \theta_k)$ and $F_\Delta(\theta_t) = F(\theta_t + \theta_k) - F(\theta_t - \theta_k)$ are the sum and difference beam patterns, respectively. When the target angle is near the equal-signal axis, i.e., $\theta = \theta_0$ ($\theta_t = 0$), performing a first-order Taylor series expansion on the above equation yields:

$$F(\theta_t + \theta_k) \approx F(\theta_t) + F'(\theta_t)\theta_t, \tag{22}$$

$$F(\theta_t - \theta_k) \approx F(\theta_t) - F'(\theta_t)\theta_t. \tag{23}$$

Thus, the ratio of the sum to the difference beam received signals can be obtained as follows:

$$\frac{u_\Delta(\theta_t)}{u_\Sigma(\theta_t)} \approx \frac{F'(\theta_t)}{F(\theta_t)}\theta_t = \rho\theta_t, \tag{24}$$

where $\rho = F'(\theta_t)/F(\theta_t)$ is the normalized slope coefficient of the beam pattern at the pointing direction. It can be seen that the ratio of sum to difference beam received signals is proportional to the deviation angle θ_t between the true target and the equal-signal axis. Therefore, it can be used to further correct the preliminary angle estimate determined by DFT codewords.

The complexity of the proposed interference detection method includes two parts. The first is the complexity of frequency domain detection, which is primarily dependent on the total number of frequency points to be scanned and the number of required iterations of the FCME algorithm. On the other hand, the complexity of the space domain detection is mainly determined by the number of active users, the number of BS and UE scanning beams, and the precision requirements of the angle-comparison table. In general, the overall latency of the whole process is reliably less than 100 μs, which can successfully adapt to high-dynamic UAV scenarios.

V. Simulation Results

To evaluate the effectiveness of the proposed FCME-based interference detection scheme, we conduct Monte Carlo simulations focusing on frequency-domain and beam-domain interference detection performance. The simulations also assess the angle estimation accuracy of the sum-difference amplitude comparison method for both interferers and affected users.

Fig. 5 illustrates the FCME-based interference detection results in both frequency and beam domains under full beam scanning. The simulation setup assigns 13 independent RBs to each user, with the interferer targeting the RBs occupied by the last five users. The left subfigure shows the distribution of detection statistics across different PRBs and the interference detection results. It is evident that the latter half of the PRBs are affected by the interferer, and the proposed algorithm successfully identifies interference presence at medium-to-high jamming-to-noise ratios (JNRs). For the undetected PRBs within the interfered frequency band, the interference power is negligible as it is comparable to the noise floor. The right subfigure presents the detection statistics distribution and interference detection results across different scanning beams. Due to the scenario configuration and the interferer's beam direction, a significant peak appears only at one specific beam. Consequently, the proposed algorithm detects a single peak, whose corresponding elevation and azimuth angles provide a coarse estimate of the interferer's

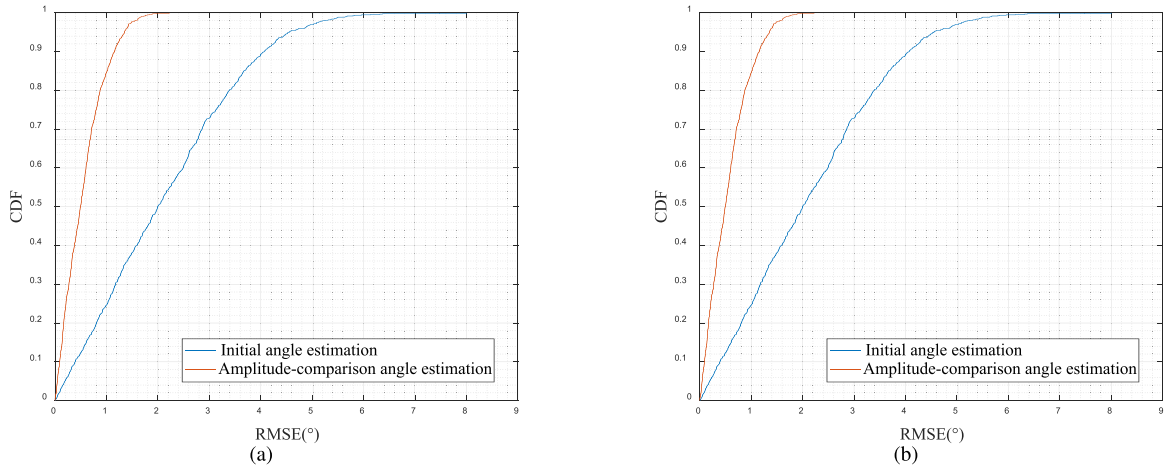

Fig. 6. CDF of RMSE for interferer azimuth and elevation angle estimation over 1000 experiments.

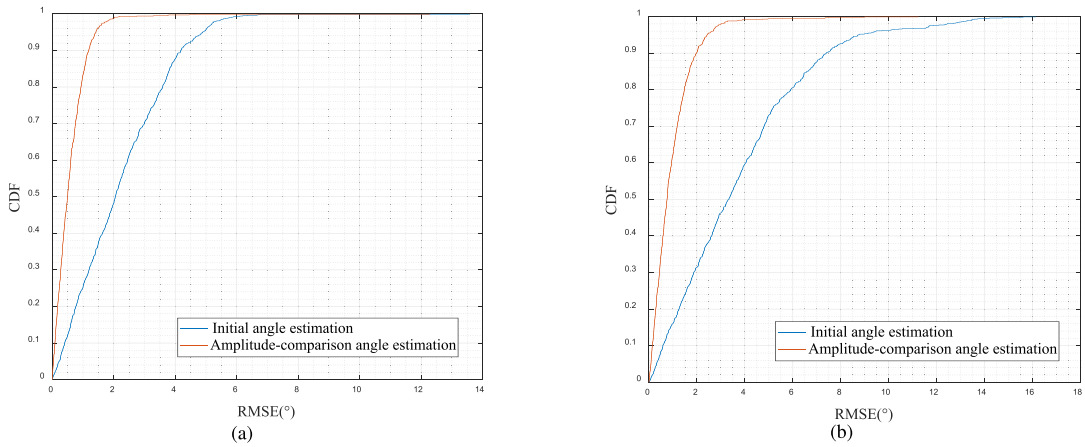

Fig. 7. CDF of RMSE for affected user azimuth and elevation angle estimation over 1000 experiments.

angle of arrival (AoA). For cases with non-negligible beam sidelobe gain or power leakage caused by misalignment between the interferer's transmission beam and the base station's reception beam, the algorithm's offset can be adjusted to fine-tune the detection threshold for precise interference localization. In scenarios with multiple interferers, a sliding window filter can be applied to the detection statistics, retaining only the peak within each window to mitigate the impact of beam sidelobes.

After performing FCME-based interference detection on the redundant pilot projected signals, the beam codewords corresponding to the interference detection results provide initial angle estimates of the interferer. The sum-difference amplitude ratio method is then employed to estimate angle deviations, further refining the interferer's angle estimation. Similarly, angle estimates for users can be obtained using the projected signals of utilized pilots. To evaluate the angle measurement performance for both interferers and users, 1000 Monte Carlo experiments were conducted. Figs. 6 and 7 show the CDFs of angle estimation errors for the interferer and the affected user, respectively. In the experiments, the correction grid for the sum-difference amplitude ratio method was set to 10, and user number 20 was selected, experiencing full-band interference. The results demonstrate that for both interferers and affected users, the proposed angle estimation method with sum-difference amplitude ratio correction significantly outperforms the initial angle estimation. Taking the interferer's azimuth estimation as an example, the initial method controls estimation errors within 4° with 90% probability over 1000 experiments, while the corrected method reduces this to 1.2° with the same probability. Additionally, due to the non-uniform resolution of the DFT codebook across different physical angles, the elevation estimation performance is slightly inferior to the azimuth estimation in simulations. Practical applications should carefully consider the potential distribution areas of targets and interferers when designing base station locations.

VI. Conclusion

In this paper, we proposed a cloud-edge-end architecture-based CF-mMIMO communication system for robust communication in UAV swarm perception networks. We first designed a hierarchical cloud-edge-end collaborative architecture that achieves scalable baseband processing and user-centric coordination through function separation between EDUs and

UCDUs. This hybrid framework effectively balances distributed efficiency and centralized coordination, addressing the backhaul overhead and processing complexity issues faced by traditional CF-mMIMO systems. Furthermore, we proposed a two-layer hybrid signal detection scheme that combines local MMSE detection at the EDU with global signal aggregation at the UCDU, maintaining near-optimal performance while reducing overhead. To tackle the dynamic interference in UAV swarm communications, we also developed a spatiotemporal-frequency FCME-based interference detection framework, which can accurately sense and locate interference sources and effectively suppress both narrowband and wideband interference. Future work will further explore the application of this architecture in multi-UAV collaborative tasks and investigate how to integrate more intelligent sensing functionalities into the cloud-edge-end framework to achieve a higher level of task collaboration and environmental awareness. Forthemore, the real-world deployment of the interfernce detction method and the performance comparison between our proposed method and machine learning-based methods are also valueable.

REFERENCES

[1] W. Xu, Z. Yang, D. W. K. Ng, M. Levorato, Y. C. Eldar, and M. Debbah, "Edge learning for B5G networks with distributed signal processing: Semantic communication, edge computing, and wireless sensing," *IEEE J. Sel. Topics Signal Process.*, vol. 17, no. 1, pp. 9–39, Jan. 2023.

[2] A. Alkhateeb, O. El Ayach, G. Leus, and R. W. Heath, "Hybrid precoding for millimeter wave cellular systems with partial channel knowledge," in *Proc. Inf. Theory Appl. Workshop*, 2013, pp. 1–5.

[3] Y. Shi, K. An, and Y. Li, "Index modulation based frequency hopping: Anti-jamming design and analysis," *IEEE Trans. Veh. Technol.*, vol. 70, no. 7, pp. 6930–6942, Jul. 2021.

[4] J. Yao, W. Xu, Z. Yang, X. You, M. Bennis, and H. V. Poor, "Wireless federated learning over resource-constrained networks: Digital versus analog transmissions," *IEEE Trans. Wireless Commun.*, vol. 23, no. 10, pp. 14020–14036, Oct. 2024.

[5] M. Campion, P. Ranganathan, and S. Faruque, "UAV swarm communication and control architectures: A review," *J. Unmanned Veh. Syst.*, vol. 7, no. 2, pp. 93–106, 2018.

[6] Y. Alqudsi and M. Makaraci, "UAV swarms: Research, challenges, and future directions," *J. Eng. Appl. Sci.*, vol. 72, no. 1, 2025, Art. no. 12.

[7] I. Chandran and K. Vipin, "Multi-UAV networks for disaster monitoring: Challenges and opportunities from a network perspective," *Drone Syst. Appl.*, vol. 12, pp. 1–28, 2024.

[8] T. L. Marzetta, "Noncooperative cellular wireless with unlimited numbers of base station antennas," *IEEE Trans. Wireless Commun.*, vol. 9, no. 11, pp. 3590–3600, Nov. 2010.

[9] T.-N. Tran and G. Interdonato, "Energy efficiency optimization in integrated satellite-terrestrial UAV-enabled cell-free massive MIMO," in *Proc. IEEE 25th Int. Workshop Signal Process. Adv. Wireless Commun.*, 2024, pp. 711–715.

[10] Y. Jiang, Q. Wu, W. Chen, and K. Meng, "UAV-enabled integrated sensing and communication: Tracking design and optimization," *IEEE Commun. Lett.*, vol. 28, no. 5, pp. 1024–1028, May 2024.

[11] X. Xiong, C. Sun, W. Ni, and X. Wang, "Three-dimensional trajectory design for unmanned aerial vehicle-based secure and energy-efficient data collection," *IEEE Trans. Veh. Technol.*, vol. 72, no. 1, pp. 664–678, Jan. 2023.

[12] H. Huang et al., "Deep learning for physical-layer 5G wireless techniques: Opportunities, challenges and solutions," *IEEE Wireless Commun.*, vol. 27, no. 1, pp. 214–222, Feb. 2020.

[13] H. Wang, W. Lyu, P. Yao, X. Liang, and C. Liu, "Three-dimensional path planning for unmanned aerial vehicle based on interfered fluid dynamical system," *Chin. J. Aeronaut.*, vol. 28, no. 1, pp. 229–239, 2015.

[14] D. Tse and P. Viswanath, *Fundamentals of Wireless Communication*. Cambridge, U.K.: Cambridge Univ. Press, 2005.

[15] A. Goldsmith, *Wireless Communications*. Cambridge, U.K.: Cambridge Univ. Press, 2005.

[16] R. W. Heath, N. Gonzalez-Prelcic, S. Rangan, W. Roh, and A. M. Sayeed, "An overview of signal processing techniques for millimeter wave MIMO systems," *IEEE J. Sel. Topics Signal Process.*, vol. 10, no. 3, pp. 436–453, Apr. 2016.

[17] L. Lu, G. Y. Li, A. L. Swindlehurst, A. Ashikhmin, and R. Zhang, "An overview of massive MIMO: Benefits and challenges," *IEEE J. Sel. Topics Signal Process.*, vol. 8, no. 5, pp. 742–758, Oct. 2014.

[18] E. Björnson, E. G. Larsson, and T. L. Marzetta, "Massive MIMO: Ten myths and one critical question," *IEEE Commun. Mag.*, vol. 54, no. 2, pp. 114–123, Feb. 2016.

[19] J. Sun, W. Shi, J. Yao, W. Xu, D. Wang, and Y. Cao, "UAV-based intelligent sensing over CF-mMIMO communications: System design and experimental results," *IEEE Open J. Commun. Soc.*, vol. 6, pp. 3211–3221, 2025.

[20] W. Shi et al., "Combating interference for over-the-air federated learning: A statistical approach via ris," *IEEE Trans. Signal Process.*, vol. 73, pp. 936–953, 2025.

[21] J. Sun, H. Lin, W. Shi, W. Xu, and D. Wang, "CF-MMIMO-based computational offloading for UAV swarms: System design and experimental results," *Electronics*, vol. 14, no. 13, 2025, Art. no. 2708.

[22] W. Shi, J. Xu, W. Xu, C. Yuen, A. L. Swindlehurst, and C. Zhao, "On secrecy performance of RIS-assisted MISO systems over Rician channels with spatially random eavesdroppers," *IEEE Trans. Wireless Commun.*, vol. 23, no. 8, pp. 8357–8371, Aug. 2024.

[23] H. Q. Ngo, A. Ashikhmin, H. Yang, E. G. Larsson, and T. L. Marzetta, "Cell-free massive MIMO versus small cells," *IEEE Trans. Wireless Commun.*, vol. 16, no. 3, pp. 1834–1850, Mar. 2017.

[24] H. Masoumi and M. J. Emadi, "Performance analysis of cell-free massive MIMO system with limited fronthaul capacity and hardware impairments," *IEEE Trans. Wireless Commun.*, vol. 19, no. 2, pp. 1038–1053, Feb. 2020.

[25] Z. H. Shaik and Erik G. Larsson, "Distributed signal processing for cell-free massive MIMO," in *Proc. IEEE Int. Conf. Acoust. Speech Signal Process.*, 2023.

[26] H. Q. Ngo, A. Ashikhmin, H. Yang, E. G. Larsson, and T. L. Marzetta, "Cell-free massive MIMO: Uniformly great service for everyone," in *Proc. IEEE 16th Int. Workshop Signal Process. Adv. Wireless Commun.*, 2015, pp. 201–205.

[27] F. Moradi, V. Hakami, and S. V. Azhari, "Resource allocation in cell-free massive MIMO networks with hybrid energy supplies," *IEEE Access*, vol. 11, pp. 47448–47468, 2023.

[28] M. Satyanarayanan, "The emergence of edge computing," *Computer*, vol. 50, no. 1, pp. 30–39, Jan. 2017.

[29] J. Park, S. Samarakoon, M. Bennis, and M. Debbah, "Wireless network intelligence at the edge," *Proc. IEEE*, vol. 107, no. 11, pp. 2204–2239, Nov. 2019.

[30] H. Dahrouj et al., "An overview of machine learning-based techniques for solving optimization problems in communications and signal processing," *IEEE Access*, vol. 9, pp. 74908–74938, 2021.

[31] Q. Peng, J. Li, and H. Shi, "Deep learning based channel estimation for OFDM systems with doubly selective channel," *IEEE Commun. Lett.*, vol. 26, no. 9, pp. 2067–2071, Sep. 2022.

[32] D. C. Nguyen et al., "6G Internet of Things: A comprehensive survey," *IEEE Internet Things J.*, vol. 9, no. 1, pp. 359–383, Jan. 2022.

[33] H. Xue, B. Huang, M. Qin, H. Zhou, and H. Yang, "Edge computing for Internet of Things: A survey," in *Proc. Int. Conf. Internet Things IEEE Green Comput. Commun. IEEE Cyber, Phys. Soc. Comput. IEEE Smart Data IEEE Congr. Cybermatics*, 2020, pp. 755–760.

[34] H. F. Shahid, B. Akdemir, J. Islam, I. Ahmad, and E. Harjula, "IoT service orchestration in edge-cloud continuum with 6G: A review," Authorea Preprints, 2025.

[35] R. He et al., "5G for railways: Next generation railway dedicated communications," *IEEE Commun. Mag.*, vol. 60, no. 12, pp. 130–136, Dec. 2022.

[36] T. S. Rappaport, F. Gutierrez, E. Ben-Dor, J. N. Murdock, Y. Qiao, and J. I. Tamir, "Broadband millimeter-wave propagation measurements and models using adaptive-beam antennas for outdoor urban cellular communications," *IEEE Trans. Antennas Propag.*, vol. 61, no. 4, pp. 1850–1859, Apr. 2013.

[37] S. Rangan, T. S. Rappaport, and E. Erkip, "Millimeter-wave cellular wireless networks: Potentials and challenges," *Proc. IEEE*, vol. 102, no. 3, pp. 366–385, Mar. 2014.

[38] J. Xu, Y. Zeng, and R. Zhang, "UAV-enabled wireless power transfer: Trajectory design and energy optimization," *IEEE Trans. Wireless Commun.*, vol. 17, no. 8, pp. 5092–5106, Aug. 2018.

[39] P. X. Nguyen, H. V. Nguyen, V.-D. Nguyen, and O.-S. Shin, "UAV-enabled cooperative jamming for physical layer security in cognitive radio network," in *Autonomous Airborne Wireless Networks*. Hoboken, NJ, USA: Wiley-IEEE Press, 2021, pp. 119–140.
[40] L. Xie, J. Xu, and R. Zhang, "Throughput maximization for uav-enabled wireless powered communication networks," *IEEE Internet Things J.*, vol. 6, no. 2, pp. 1690–1703, Apr. 2019.
[41] X. Wang et al., "A survey on security of UAV swarm networks: Attacks and countermeasures," *ACM Comput. Surv.*, vol. 57, no. 3, pp. 1–37, 2024.
[42] M. Z. Hassan, G. Kaddoum, and O. Akhrif, "Resource allocation for joint interference management and security enhancement in cellular-connected Internet-of-Drones networks," *IEEE Trans. Veh. Technol.*, vol. 71, no. 12, pp. 12869–12884, Dec. 2022.
[43] W. Cheng, Z. Li, F. Gao, L. Liang, and H. Zhang, "Mode hopping for anti-jamming in cognitive radio networks," in *Proc. IEEE/CIC Int. Conf. Commun. China*, 2018, pp. 530–535.
[44] J.-F. Huang, G.-Y. Chang, and J.-X. Huang, "Anti-jamming rendezvous scheme for cognitive radio networks," *IEEE Trans. Mobile Comput.*, vol. 16, no. 3, pp. 648–661, Mar. 2017.
[45] L. Luo, J. Zhang, S. Chen, X. Zhang, B. Ai, and D. W. K. Ng, "Downlink power control for cell-free massive MIMO with deep reinforcement learning," *IEEE Trans. Veh. Technol.*, vol. 71, no. 6, pp. 6772–6777, Jun. 2022.
[46] E. A. Lee and D. G. Messerschmitt, *Digital Communication*. Berlin, Germany: Springer, 2012.
[47] A. J. Viterbi, *CDMA: Principles of Spread Spectrum Communication*. Reading, MA, USA: Addison-Wesley, 1995.
[48] N. Li et al., "Spatial sparsity-based pilot attack detection and transmission countermeasure for cell-free massive MIMO system," *IEEE Syst. J.*, vol. 17, no. 2, pp. 2065–2076, Jun. 2023.
[49] A. Abdallah and M. M. Mansour, "Angle-based multipath estimation and beamforming for FDD cell-free massive MIMO," in *Proc. IEEE 20th Int. Workshop Signal Process. Adv. Wireless Commun.*, 2019, pp. 1–5.
[50] L. A. Iliadis, Z. D. Zaharis, S. Sotiroudis, P. Sarigiannidis, G. K. Karagiannidis, and S. K. Goudos, "The road to 6G: A comprehensive survey of deep learning applications in cell-free massive MIMO communications systems," *EURASIP J. Wireless Commun. Netw.*, vol. 2022, no. 1, 2022, Art. no. 68.
[51] E. G. Larsson, O. Edfors, F. Tufvesson, and T. L. Marzetta, "Massive MIMO for next generation wireless systems," *IEEE Commun. Mag.*, vol. 52, no. 2, pp. 186–195, Feb. 2014.
[52] T. L. Marzetta, "Massive MIMO: An introduction," *Bell Labs Tech. J.*, vol. 20, pp. 11–22, 2015.
[53] Y. Zeng, R. Zhang, and T. J. Lim, "Throughput maximization for UAV-enabled mobile relaying systems," *IEEE Trans. Commun.*, vol. 64, no. 12, pp. 4983–4996, Dec. 2016.
[54] C. D'Andrea, A. Garcia-Rodriguez, G. Geraci, L. G. Giordano, and S. Buzzi, "Cell-free massive MIMO for UAV communications," in *Proc. IEEE Int. Conf. Commun. Workshops*, 2019, pp. 1–6.
[55] S. Kim and S. Jeon, "Fronthaul compression and beamforming optimization for secure cell-free ISAC systems," *IEEE Wireless Commun. Lett.*, vol. 14, no. 12, pp. 3847–3851, Dec. 2025.
[56] D. Wang, C. Zhang, Y. Du, J. Zhao, M. Jiang, and X. You, "Implementation of a cloud-based cell-free distributed massive MIMO system," *IEEE Commun. Mag.*, vol. 58, no. 8, pp. 61–67, Aug. 2020.
[57] Y. Guo et al., "Stochastic geometry analysis of scalable cell-free ran with dynamic association and deployment," *IEEE J. Sel. Topics Signal Process.*, vol. 19, no. 2, pp. 398–411, Mar. 2025.
[58] M. Zaher, E. Björnson, and M. Petrova, "Soft handover procedures in mmWave cell-free massive MIMO networks," *IEEE Trans. Wireless Commun.*, vol. 23, no. 6, pp. 6124–6138, Jun. 2024.
[59] N. Abbas, Y. Zhang, A. Taherkordi, and T. Skeie, "Mobile edge computing: A survey," *IEEE Internet Things J.*, vol. 5, no. 1, pp. 450–465, Feb. 2018.
[60] W. Z. Khan, E. Ahmed, S. Hakak, I. Yaqoob, and A. Ahmed, "Edge computing: A survey," *Future Gener. Comput. Syst.*, vol. 97, pp. 219–235, 2019.
[61] N. Hassan, K.-L. A. Yau, and C. Wu, "Edge computing in 5G: A review," *IEEE Access*, vol. 7, pp. 127276–127289, 2019.
[62] M. Almusawi, M. Balakrishnan, V. D. Babu, S. S. Naveena, A. Sharma, and S. SubbaRao, "Implementation of 5G cloud based technique development using radio access type of networks," in *Proc. 4th Int. Conf. Adv. Comput. Innov. Technol. Eng.*, 2024, pp. 422–426.
[63] D. Wubben et al., "Benefits and impact of cloud computing on 5G signal processing: Flexible centralization through cloud-RAN," *IEEE Signal Process. Mag.*, vol. 31, no. 6, pp. 35–44, Nov. 2014.
[64] M.-T. Lee, M.-L. Chuang, S.-T. Kuo, and Y.-R. Chen, "UAV swarm real-time rerouting by edge computing d* lite algorithm," *Appl. Sci.*, vol. 12, no. 3, 2022, Art. no. 1056.
[65] S. Mukherjee and J. Lee, "Edge computing-enabled cell-free massive MIMO systems," *IEEE Trans. Wireless Commun.*, vol. 19, no. 4, pp. 2884–2899, Apr. 2020.
[66] Z. Hu, S. Liu, D. Zhou, C. Shen, and T. Wang, "Task offloading and data compression collaboration optimization for UAV swarm-enabled mobile edge computing," *Drones*, vol. 9, no. 4, 2025, Art. no. 288.
[67] C. Ding, A. Zhou, Y. Liu, R. N. Chang, C.-H. Hsu, and S. Wang, "A cloud-edge collaboration framework for cognitive service," *IEEE Trans. Cloud Comput.*, vol. 10, no. 3, pp. 1489–1499, Jul.–Sep. 2022.
[68] L. Zhang, J. Peng, J. Zheng, and M. Xiao, "Intelligent cloud-edge collaborations assisted energy-efficient power control in heterogeneous networks," *IEEE Trans. Wireless Commun.*, vol. 22, no. 11, pp. 7743–7755, Nov. 2023.
[69] T. I. Ahmed and H. N. M. Ali, "Problems and solutions of frequency hopping for drones: A review," *Al-Furat J. Innovations Electron. Comput. Eng.*, vol. 4, no. 1, pp. 34–50, 2025.
[70] R. Xue and M. Zhao, "Cognitive-based high robustness frequency hopping strategy for UAV swarms in complex electromagnetic environment," *Wireless Commun. Mobile Comput.*, vol. 2022, no. 1, 2022, Art. no. 4139345.
[71] C. Shen, T.-H. Chang, J. Gong, Y. Zeng, and R. Zhang, "Multi-UAV interference coordination via joint trajectory and power control," *IEEE Trans. Signal Process.*, vol. 68, pp. 843–858, 2020.
[72] N. R. R. et al., "UAV-based cell-free massive MIMO: Joint activation and power optimization under fronthaul capacity limitations," *IEEE Wireless Commun. Lett.*, vol. 14, no. 8, pp. 2496–2500, Aug. 2025.
[73] W. Miao, C. Luo, G. Min, and Z. Zhao, "Lightweight 3-D beamforming design in 5G UAV broadcasting communications," *IEEE Trans. Broadcast.*, vol. 66, no. 2, pp. 515–524, Jun. 2020.
[74] E. V. Pothan and S. Kashyap, "Cell-free massive MIMO enabled wireless communication with UAVs in underlay spectrum access networks," *IEEE Trans. Commun.*, vol. 71, no. 12, pp. 7363–7377, Dec. 2023.
[75] H. Wang, Q. Chang, and Y. Wang, "A digital beamforming anti-jamming method based on signal eigen-subspace," *IEEE Commun. Lett.*, vol. 29, no. 2, pp. 240–243, Feb. 2025.
[76] R. Vuohtoniemi, J.-P. Mäkelä, J. Vartiainen, and J. Iinatti, "Detection of broadcast signals in cognitive radio based PLC using the FCME algorithm," in *Proc. 18th IEEE Int. Symp. Power Line Commun. Appl.*, 2014, pp. 70–74.
[77] J. J. Lehtomäki, J. Vartiainen, R. Vuohtoniemi, and H. Saarnisaari, "Adaptive fcme-based threshold setting for energy detectors," in *Proc. 4th Int. Conf. Cogn. Radio Adv. Spectr. Manage.*, 2011, pp. 1–5.
[78] Z. Zhang, Z. Deng, and Z. Ding, "Interference detection method based on DTFRFT-FCME and joint multi-threshold judgment," in *Proc. IEEE 10th Int. Conf. Comput. Sci. Netw. Technol.*, 2022, pp. 132–139.
[79] B. Wang, A. Li, A. Wang, Y. Sun, and S. Li, "Data-knowledge-driven for UAV swarm communication interference recognition," *IEEE Internet Things J.*, vol. 12, no. 21, pp. 43978–43990, Nov. 2025.
[80] H. Hosseini and E. Aryafar, "Ai-based interference pattern prediction and fair scheduling in full-duplex wireless IoT networks," in *Proc. IEEE World AI IoT Congr.*, 2025, pp. 0497–0506.
[81] Z. Hong, T. Li, C. Li, D. Wang, and X. You, "Group-joint MMSE complementary-based distributed uplink for cell-free massive MIMO," *IEEE Trans. Wireless Commun.*, vol. 23, no. 10, pp. 13648–13663, Oct. 2024.
[82] D. Wanget al., "Full-spectrum cell-free ran for 6G systems: System design and experimental results," *Sci. China Inf. Sci.*, vol. 66, no. 3, 2023, Art. no. 130305.

Jian Sun received M.S. degree from Beihang University, Beijing, China in 2016. He is currently working toward the Doctor of Philosophy (Ph.D.) degree in electronic and information engineering with the National Mobile Communications Research Laboratory, Southeast University, Nanjing, China. From 2016 to 2021, he joined Military Engineering Department, 28th Research Institute of China Electronics Technology Group Corporation (CETC), as a Project Manager. In 2022, he joined the Pervasive Communication Research Center, Purple Mountain Laboratory, Nanjing, China, as a Key Scientific Research Engineer. His research interests include cell-free massive multiple-input multiple-output (MIMO) systems, unmanned systems, and communication-sensing integrated systems.

Dongxuan He (Member, IEEE) received the B.S. degree in automation and the Ph.D. degree in information and communication systems from the Beijing Institute of Technology (BIT), Beijing, China, in 2013 and 2019, respectively. From 2017 to 2018, he was a Visiting Student with the Singapore University of Technology and Design (SUTD), Singapore. From 2019 to 2022, he was a Postdoctoral Researcher with the Department of Electronic Engineering, Tsinghua University, Beijing. He is currently an Assistant Professor with the School of Information and Electronics, BIT. His current interests include Integrated sensing and communication (ISAC), terahertz communication, and AI empowered wireless communications. He is also the Guest Editor of IEEE OPEN JOURNAL OF THE COMMUNICATIONS SOCIETY, *Electronics*, and *Space: Science & Technology*. He is a TPC member of various flagship IEEE conferences, such as IEEE ICC and IEEE GLOBECOM. He was the recipient of the Best Paper Award from 2024 IEEE ICSIDP and 2025 IEEE IWCMC. He was also an Exemplary Reviewer of IEEE WIRELESS COMMUNICATIONS LETTERS.

Huazhou Hou (Member, IEEE) received the B.S. degree from the Beijing Institute of Technology (BIT), Beijing, China, in 2013, and the M.S. and Ph.D. degrees from Northeast University, Boston, MA, USA, in 2015 and 2020, respectively. From 2017 to 2019, he was a joint Ph.D. Student with RMIT University, Melbourne, VIC, Australia. From 2020 to 2023, he was a Postdoctoral with Southeast University, Nanjing, China. He is currently an Associate Professor with Purple Mountain Laboratories, Nanjing, China. His research interests include AI-native wireless communication, integrated sensing and communication (ISAC), and signal processing.

Pengguang Du (Graduate Student Member, IEEE) received the B.Eng. degree in communication engineering from Jilin University, Changchun, China, in 2021. He is currently working toward the Ph.D. degree in information and communication engineering with the School of Information Science and Engineering, Southeast University, Nanjing, China. His research interests include massive MIMO channel acquisition and intelligent wireless communications.

Chao Fang (Graduate Student Member, IEEE) received the M.S. degree in communication engineering from the University of Electronic Science and Technology of China, Chengdu, China, in 2023. He is currently working toward the Ph.D. degree in information and communication engineering with the School of Information Science and Engineering, Southeast University, Nanjing, China. His current research interests include radio resource management and intelligent wireless communications.

Changwei Zhang (Member, IEEE) received the M.S. degree in electronics and communication engineering and the Ph.D. degree in communication and information system from the Nanjing University of Posts and Telecommunications (NJUPT), Nanjing, China, in 2018 and 2021, respectively, and the second Ph.D. degree in electrical and computer engineering from Western University, London, ON, Canada, in 2023. He is currently a Postdoctoral Researcher with Purple Mountain Laboratories. His research interests include Internet-of-Things, random access, machine learning, and mmWave communications.

Wei Xu (Fellow, IEEE) received the B.Sc. degree in electrical engineering, and the M.S. and Ph.D. degrees in communication and information engineering from Southeast University, Nanjing, China, in 2003, 2006, and 2009, respectively. From 2009 to 2010, he was a Postdoctoral Research Fellow with the University of Victoria, Victoria, BC, Canada. He was an Adjunct Professor with the University of Victoria from 2017 to 2020 and Distinguished Visiting Fellow with the Royal Academy of Engineering, London, U.K., in 2019. He is currently a Professor with Southeast University, Nanjing, China. His research interests include information theory, signal processing, and artificial intelligence for wireless communications. He was the recipient of the Science and Technology Award for Young Scholars of the China Institute of Communications in 2018, Science and Technology Award of the Chinese Institute of Electronics (Second Prize) in 2019, National Natural Science Foundation of China for Outstanding Young Scholars in 2020, IEEE Communications Society Heinrich Hertz Award in 2023, and Best Paper Awards at IEEE ICC 2024, IEEE Globecom 2014, IEEE ICCC 2014, ISWCS 2018, and WCSP 2017 and 2021, respectively. He was the Editor of IEEE TRANSACTIONS ON COMMUNICATIONS from 2018 to 2023, and Editor and Senior Editor of IEEE COMMUNICATIONS LETTERS from 2015 to 2023. He is Area Editor of IEEE COMMUNICATIONS LETTERS and Associate Editor for IEEE TRANSACTIONS ON VEHICULAR TECHNOLOGY. He is a fellow of IET.

Dongming Wang (Member, IEEE) received the B.S. degree from the Chongqing University of Posts and Telecommunications, Chongqing, China, in 1999, the M.S. degree from the Nanjing University of Posts and Telecommunications, Nanjing, China, in 2002, and the Ph.D. degree from Southeast University, Nanjing, in 2006. In 2006, he joined the National Mobile Communications Research Laboratory, Southeast University, where he is currently a Professor. His research interests include signal processing for wireless communications and large-scale distributed MIMO systems (cell-free massive MIMO). Dr. Wang was the Symposium Co-Chair of 2015 IEEE International Conference on Communications (ICC 2015) and IEEE Wireless Communications and Signal Processing Conference (IEEE WCSP 2017). He is also an Associate Editor for *Science China Information Sciences*.

Yongming Huang (Fellow, IEEE) received the B.S. and M.S. degrees from Nanjing University, Nanjing, China, in 2000 and 2003, respectively, and the Ph.D. degree in electrical engineering from Southeast University, Nanjing, in 2007. During 2008–2009, he visited Signal Processing Lab, Royal Institute of Technology (KTH), Stockholm, Sweden. Since 2007, he has been a Faculty with the School of Information Science and Engineering, Southeast University, where he is currently a Full Professor. He has also been the Director of Pervasive Communication Research Center, Purple Mountain Laboratories, since 2019. He has authored or coauthored more than 200 peer-reviewed papers, hold more than 80 invention patents. He submitted around 20 technical contributions to IEEE standards, and was awarded a certificate of appreciation for outstanding contribution to the development of IEEE standard 802.11aj. His current research interests include intelligent 5G/6G mobile communications and millimeter wave wireless communications. He was an Associate Editor for IEEE TRANSACTIONS ON SIGNAL PROCESSING and Guest Editor of IEEE JOURNAL SELECTED AREAS IN COMMUNICATIONS. He is also the Editor-at-Large of IEEE OPEN JOURNAL OF THE COMMUNICATIONS SOCIETY and Associate Editor for IEEE WIRELESS COMMUNICATIONS LETTERS.